NeuroImage 52 (2010) 1162–1170

Contents lists available at ScienceDirect

NeuroImage

journal homepage: www.elsevier.com/locate/ynimg

Comments and Controversies

BOLD correlates of EEG topography reveal rapid resting-state network dynamics

Juliane Britz [a,b,*], Dimitri Van De Ville [c,d], Christoph M. Michel [a,b,e]

[a] Department of Fundamental Neuroscience, University of Geneva, Switzerland
[b] EEG Brain Mapping Core, Biomedical Imaging Center (CIBM), University of Geneva, Switzerland
[c] Department of Radiology and Medical Informatics, University of Geneva, Switzerland
[d] Institute of Bioengineering, Ecole Polytechnique Fédérale de Lausanne, Switzerland
[e] Department of Neurology, University of Geneva Medical School, Switzerland

ARTICLE INFO

Article history:
Received 22 December 2009
Revised 2 February 2010
Accepted 17 February 2010
Available online 24 February 2010

Keywords:
EEG
fMRI
EEG microstates
EEG topography
Resting state
ICA
GLM
Rapid dynamics
Resting-state networks
Default-mode network

ABSTRACT

Resting-state functional connectivity studies with fMRI showed that the brain is intrinsically organized into large-scale functional networks for which the hemodynamic signature is stable for about 10 s. Spatial analyses of the topography of the spontaneous EEG also show discrete epochs of stable global brain states (so-called microstates), but they remain quasi-stationary for only about 100 ms. In order to test the relationship between the rapidly fluctuating EEG-defined microstates and the slowly oscillating fMRI-defined resting states, we recorded 64-channel EEG in the scanner while subjects were at rest with their eyes closed. Conventional EEG-microstate analysis determined the typical four EEG topographies that dominated across all subjects. The convolution of the time course of these maps with the hemodynamic response function allowed to fit a linear model to the fMRI BOLD responses and revealed four distinct distributed networks. These networks were spatially correlated with four of the resting-state networks (RSNs) that were found by the conventional fMRI group-level independent component analysis (ICA). These RSNs have previously been attributed to phonological processing, visual imagery, attention reorientation, and subjective interoceptive–autonomic processing. We found no EEG-correlate of the default mode network. Thus, the four typical microstates of the spontaneous EEG seem to represent the neurophysiological correlate of four of the RSNs and show that they are fluctuating much more rapidly than fMRI alone suggests.

Introduction

Functional connectivity of the resting brain, i.e. coherent spontaneous fluctuations of the blood-oxygen-level dependent (BOLD) response, has been identified in a wide range of functional large-scale cortical networks, the so-called resting-state networks (RSNs). Such connectivity is conventionally assessed by correlating the low-frequency portion of the BOLD signal in a seed region with the rest of the brain (Biswal et al., 1995; Fox et al., 2005, 2006; Seeley et al., 2007; Taylor et al., 2009b). More recently, Independent Component Analysis (ICA) has become a widely used tool to analyze resting-state fMRI data. ICA is a blind source separation method that allows unmixing the unknown sources that constitute a signal such that these sources are maximally independent and without the need of prior information of the sources. It has been used to decompose the fMRI signal at rest into its constituents that are both temporally and spatially independent (Beckmann et al., 2005; Calhoun et al., 2008; Damoiseaux et al., 2006; Mantini et al., 2007; McKeown and Sejnowski, 1998).

Resting-state functional connectivity has been identified for e.g. the motor system (Biswal et al., 1995), the language system (Hampson et al., 2002), executive control and saliency processing (Seeley et al., 2007), the dorsal and ventral attention systems (Fox et al., 2006) and a network implied in processing interoceptive information with emotional salience (Taylor et al., 2009a). The hemodynamic footprint is well investigated, but the underlying electrophysiological signature remains a matter of debate (Laufs et al., 2003; Leopold et al., 2003; Mantini et al., 2007; Nir et al., 2008; Tyvaert et al., 2008).

The most puzzling aspect of resting-state functional connectivity is its slow dynamics: coherent hemodynamic fluctuations are observed in the low frequencies (<0.1 Hz) of the BOLD signal. The RSNs are temporally and spatially anti-correlated, and a given RSN dominates for about 10 s (Fox et al., 2005). However, such long durations of stable functional networks are hardly compatible with the fast fluctuations of momentary cognitive thoughts that require reorganization of different spatial patterns of coordination in a sub-second time scale (Bressler, 1995; Bressler and Tognoli, 2006). Electrophysiological recordings of brain activity with EEG or MEG confirm these rapid dynamics by showing fast fluctuations of local and global neuronal oscillations at rest. The obvious question is whether and how the slow (<0.1 Hz) BOLD fluctuations are related to

* Corresponding author. Department of Fundamental Neuroscience, Centre Medical Universitaire, 1 Rue Michel-Servet, CH-1211 Geneva, Switzerland. Fax: +41 22 379 5452.
E-mail address: Juliane.Britz@unige.ch (J. Britz).

1053-8119/$ – see front matter © 2010 Elsevier Inc. All rights reserved.
doi:10.1016/j.neuroimage.2010.02.052

the fast neuronal oscillations (1–80 Hz) seen in the EEG. Several studies directly probed the relation between EEG oscillations and BOLD activity at rest by measuring the EEG in the scanner and correlating the time course of EEG frequency power with the BOLD signal. They demonstrated significant correlations in brain regions that partly corresponded to some of the above described RSNs, albeit with somewhat heterogeneous results (Goldman et al., 2002; Jann et al., 2009; Laufs et al., 2003; Tyvaert et al., 2008). In a recent study, six RSNs were identified by means of ICA and post-hoc correlated to the power time course in the EEG frequency bands (Mantini et al., 2007). None of the resting-state networks could be linked to the power in one single frequency band but rather to profiles of EEG power in different frequency bands. Taken together, the rather complex relations between EEG oscillations and RSNs can be explained by two factors: First, neither single neurons (Llinas, 1988) nor larger networks (Buzsaki and Draguhn, 2004; Steriade, 2001) oscillate exclusively at narrow frequency bands. Second, activity in the same frequency band can be generated by different physiological mechanisms in different brain areas and can have different behavioral correlates (Bollimunta et al., 2008; Young and McNaughton, 2009). Finally, the tight phase-amplitude coupling between different EEG frequency bands (Canolty et al., 2006; Lakatos et al., 2005; Schroeder and Lakatos, 2009a) reflects a complex oscillatory hierarchy of the EEG (Schroeder and Lakatos, 2009b) which makes it difficult to distinguish the contribution of one band alone.

The EEG scalp topography is a much more direct measure of the momentary global state of the brain than the frequency power over a certain scalp area. It represents the summation of all concurrently active sources in the brain irrespective of their frequency (Koenig et al., 2002; Lehmann and Skrandies, 1980, 1984; Wackermann et al., 1993). Moreover, the EEG scalp topography remains quasi-stable for periods of about 80–120 ms; such stability is not found in amplitude and power modulations at the single electrodes. During these periods of quasi-stability, the topography remains fixed, while polarity can invert; such inversions are driven by the dominant generator oscillation. Interestingly, the scalp topographies observed at rest can be clustered into a limited number of map classes with prototypical configurations. Even more surprisingly, typically not more than four topographies are persistently identified across the entire life span (Koenig et al., 2002; Strik and Lehmann, 1993; Wackermann et al., 1993). These periods of stable EEG topography are referred to as EEG microstates (Katayama et al., 2007; Lehmann, 1990; Lehmann et al., 2009; Wackermann et al., 1993).

EEG microstates can influence cognition and perception (Britz et al., 2009; Mohr et al., 2005) and characterize qualitative aspects of spontaneous thoughts (Lehmann et al., 1998), which indicates that they index different types of mental processes. They can be thought of representing the "building blocks of cognition" or "atoms of thought" that underlie spontaneous conscious cognitive activity (Koenig et al., 2005; Lehmann et al., 1998, 2009). Since such task-independent mental operations might also generate the spontaneously fluctuating BOLD signal of the RSNs (Raichle and Snyder, 2007), it is logical to assume a direct link between EEG microstates and BOLD fluctuations at rest.

We hypothesized that RSN dynamics are much more rapid than previously assumed based on analyses of the fMRI signal alone, and that the EEG microstates are their electrophysiological signature. We concurrently recorded EEG and fMRI while subjects were resting in the scanner with their eyes closed. We identified the most dominant EEG microstates indexed by their scalp topography and used their time course to predict the BOLD signal. Our aim was to use a purely neural signal for the subsequent fMRI analysis which a) represents global brain activity independent of frequency b) has a high temporal resolution and that c) is of non-hemodynamic nature. In order to compare the BOLD-networks revealed by the EEG-microstate-informed fMRI analysis with the conventional RSN analysis based on fMRI only, we used group ICA to identify the independent sources that constitute the fMRI data. We then computed the spatial correlation of the activation maps obtained by the two methods to confirm the similarity of the RSNs.

Methods

Subjects and procedure

Nine healthy right-handed individuals participated for monetary compensation after giving informed consent approved by the University Hospital of Geneva Ethics Committee. None suffered from current or prior neurological or psychiatric impairments or claustrophobia. Mean age of participants was 28.37 years (range 24–33 years).

Subjects were lying in the scanner with their eyes closed. They were instructed to move as little as possible and to refrain from falling asleep, and three sessions of 5 min were recorded. Subsequent self-report and inspection of sleep pattern of the EEG led to the exclusion of one subject. The data of eight subjects were submitted to further analysis.

Simultaneous EEG/fMRI recording

The EEG was recorded from 64 sintered Ag/AgCl ring electrodes mounted in an elastic cap (EasyCaps, Falk Minnow Services, Herrsching, Germany) and arranged in an extended 10–10 System. Electrodes were equipped with an additional 5 kΩ in series-resistor, and impedances were kept below 15 kΩ. The EEG was acquired with a band-pass filter between 0.1 Hz and 250 Hz and digitized at 5 kHz, referenced online to FCz using a non-magnetic MRI-compatible EEG system (BrainAmp MR plus, Brainproducts, Munich, Germany). The ECG was recorded from a bilateral montage above and below the heart from sintered Ag/AgCl electrodes with an additional 15 kΩ resistor and digitized like the scalp EEG using a BrainAmp ExG MR amplifier. The EEG amplifier along with a rechargeable power pack was placed ca. 15 cm outside the bore. The amplified and digitized EEG signal was transmitted to the recording computer placed outside the scanner room via fiber optic cables.

Anatomical and functional imaging was acquired using a 3 T-whole body scanner (Siemens Magnetom Trio TIM, Erlangen, Germany) equipped with a standard birdcage headcoil. A magnetization prepared rapid acquisition gradient-echo sequence was employed to acquire high-resolution T1-weighted structural images (TR/TE/TI = 2500 ms/3 ms/1100 ms, flip angle = 3°, thickness = 0.9 mm, acquisition matrix 256 × 240, in-plane resolution = 0.89 × 0.89 mm^2). Functional volumes, comprising 25 slices (thickness = 5 mm + 0.5 mm gap) parallel to the AC–PC line, were obtained using a multislice gradient-echo planar imaging (EPI) sequence (TR/TE = 1500 ms/35 ms, flip angle = 90°, acquisition matrix 64 × 64, in-plane resolution 3.75 × 3.75 mm^2, FOV = 240 × 240 mm). In total 3 runs were performed, each consisting of 200 volumes, yielding a total of 600 functional volumes. Slice acquisition was performed continuously in order to facilitate off-line gradient artifact correction of the EEG.

EEG data processing

In a first step, the gradient artifacts were removed using a sliding average (Allen et al., 2000) of 21 averages and subsequently, the EEG was downsampled to 500 Hz and low-pass filtered with an IIR filter with a cut-off frequency of 70 Hz. Subsequently, the ballistocardiogram (BCG) artifact was removed by first using a sliding average procedure with 11 averages (Allen et al., 1998) and then applying ICA in order to remove residual BCG along with oculo-motor components. The so-cleaned EEG was then band-pass filtered between 1 and 40 Hz and further downsampled to 125 Hz, and the maxima of the Global Field Power (GFP) were determined. Since topography remains stable around peaks of the GFP, they are the best

representative of the momentary map topography in terms of signal-to-noise ratio (Koenig et al., 2002). All maps marked as GFP peaks (i.e. the voltage values at all electrodes at that time point) were extracted and submitted to a modified spatial cluster analysis using the Atomize-Agglomerate Hierarchical (AAHC) clustering method (Tibshirani and Walther, 2005) in order to identify the most dominant map topographies (Britz et al., 2009). The optimal number of template maps was determined by means of a cross-validation criterion (Pascual-Marqui et al., 1995). The cross-validation criterion is a measure about the residual variance, and it identifies the best solution to a cluster analysis. In other words, the cross-validation criterion identified the minimal number of template maps that explain the maximal variance. We made no a-priori assumptions on the number of clusters or on the minimum of explained variance, because we wanted our analysis to be strictly data-driven.

We then submitted the template maps identified in every single subject into a second AAHC cluster analysis to identify the dominant clusters across all subjects. Finally, we computed a spatial correlation between the templates identified at the group level with those identified for each subject in every run. We so labeled each individual map with the group template it best corresponded to in order to use the same labels for the subsequent group analysis. We will use the terms “scalp map” and “topography” interchangeably throughout the manuscript to refer to the topographical configuration of the momentary EEG scalp potential field and “template map” to refer to template maps identified in the cluster analysis.

We computed the spatial correlation between the EEG and each of the template maps, i.e. for each template map we obtained a measure of how well it explained the topography of the EEG at every moment in time (Murray et al., 2008). This yielded the time course of the microstates. In order to assure that none of the microstates reflected the ballistocardiogram, we computed the correlation of the time courses of the microstates and the ECG for each run of each subject. In every single run, there was no correlation between the time courses of the microstates and the ECG. These spatial correlation time courses were then used for subsequent fMRI data analysis.

In order to investigate whether the identified topographies might be related to activity in different frequency bands, we performed time-frequency analysis (S-Transform) for the delta (1–4 Hz), theta (4–8 Hz), alpha (8–14 Hz), beta (14–20 Hz), and gamma (20–40 Hz) frequency bands and calculated the average power across all channels at each moment in time for the five frequency bands. We then computed the cross-correlation matrix (Pearson's R) between the time courses of frequency power and the time courses of the spatial correlations of each template map. This yielded (i) how strongly the time courses of the momentary scalp topographies, (ii) the power in the five frequency bands and (iii) the time courses of the momentary scalp topographies and the frequency powers correlate with each other.

FMRI data processing

Spatial pre-processing and GLM analysis

Image pre-processing and statistical analyses were performed using the SPM5 software (Wellcome Department of Imaging Neuroscience, London, UK). First, all functional volumes were spatially realigned to the first volume, normalized into MNI space (Montreal Neurological Institute, resampled voxel size: $2\times2\times2$ mm) by using cubic B-spline interpolation, and smoothed using an isotropic Gaussian spatial kernel of FWHM = 6 mm. Since subjects moved less than 0.2 mm and less than 0.001°, we refrained from including motion parameter estimates from the realignment procedure.

For statistical analysis, the design matrix of the general linear model (GLM) was set up with custom regressors that modeled the BOLD responses associated to each microstate map. The spatial correlation time courses of each microstate map were convolved with SPM's canonical HRF. The convolution was performed on the EEG time resolution and subsequently sampled at the fMRI acquisition time-points. In other words, we build a model of how each template map could explain the BOLD fMRI activations in each subject. (See Supplementary Fig. 1 for an illustration of the procedure for the construction of the regressors.) The GLM modeling included a high-pass filter with cut-off of 1/128 Hz in order to remove low-frequency components due to scanner drifts and serial correlation was modeled by the autoregressive model of order 1. The analysis was performed for the individual subjects and also at the group level by a multi-subject GLM where we matched the regressors of the corresponding maps of the individuals. Statistical maps were obtained using t-tests and corrected for multiple comparisons using false discovery rate (FDR) at $p = 0.05$. We also performed single-subject GLM analysis (t-test, corrected, FDR at $p = 0.05$) to test for the presence of the maps at the individual level.

Group-ICA analysis

We used group spatial ICA (Calhoun et al., 2001) to decompose the data into independent components using the GIFT toolbox (http://icatb.sourceforge.net/). We estimated the number of components to be 20, and applied ICA to the group data in the following way: we concatenated all three sessions of all eight subjects and used PCA to reduce the data set to 20 temporal dimensions followed by an estimation of the independent components using the infomax algorithm (Bell and Sejnowski, 1995).

Each IC represents an idiosyncratic pattern of activity with its particular time course that is maximally independent of the other ICs. Their spatial maps represent the intensity with which the corresponding waveform is expressed at each voxel. We scaled the intensities at each voxel to z-scores (D'Argembeau et al., 2005), and those voxels exhibiting z-scores greater than 1.5 were considered as IC-active voxels (Mantini et al., 2007). Positive z-scores indicate BOLD modulations with the same time course than the IC waveform, and negative z-scores indicate BOLD modulations with opposite time courses than the IC waveform.

Comparison of GLM- and group ICA analyses

To assess spatial correlation between the activation maps identified by EEG-informed GLM analysis and ICA, we computed the normalized spatial correlation coefficients after additional smoothing using 8 mm FWHM Gaussian kernel. We then deployed a wavelet statistical resampling method (Patel et al., 2006) to determine the threshold of significant correlation for a given GLM contrast by generating a large number of surrogate volumes that maintain the spatial autocorrelation structure of the original data and by comparing the observed correlation against the maximum one for surrogates. Using $n = 399$ surrogate volumes for each GLM map results in a false positive error rate of $p = 0.05$, corrected for multiple comparisons (20 per map), the corresponding thresholds are $r = 0.25$, 0.30, 0.41, and 0.30, for each map, respectively.

Anatomical localization of the statistical results

Results of the statistical analyses were overlaid on the MNI152 average T1 weighted template available in SPM5. Their anatomical localizations were determined using the WFU pickatlas plugin for SPM5 (http://fmri.wfubmc.edu/cms/software)

Fig. 1. EEG template maps identified in every subject and each run. The cluster analysis identified four template maps as the best solution of the cluster analysis in every subject in each run. The maps are displayed with the left hemifield on the left and the nose on top.

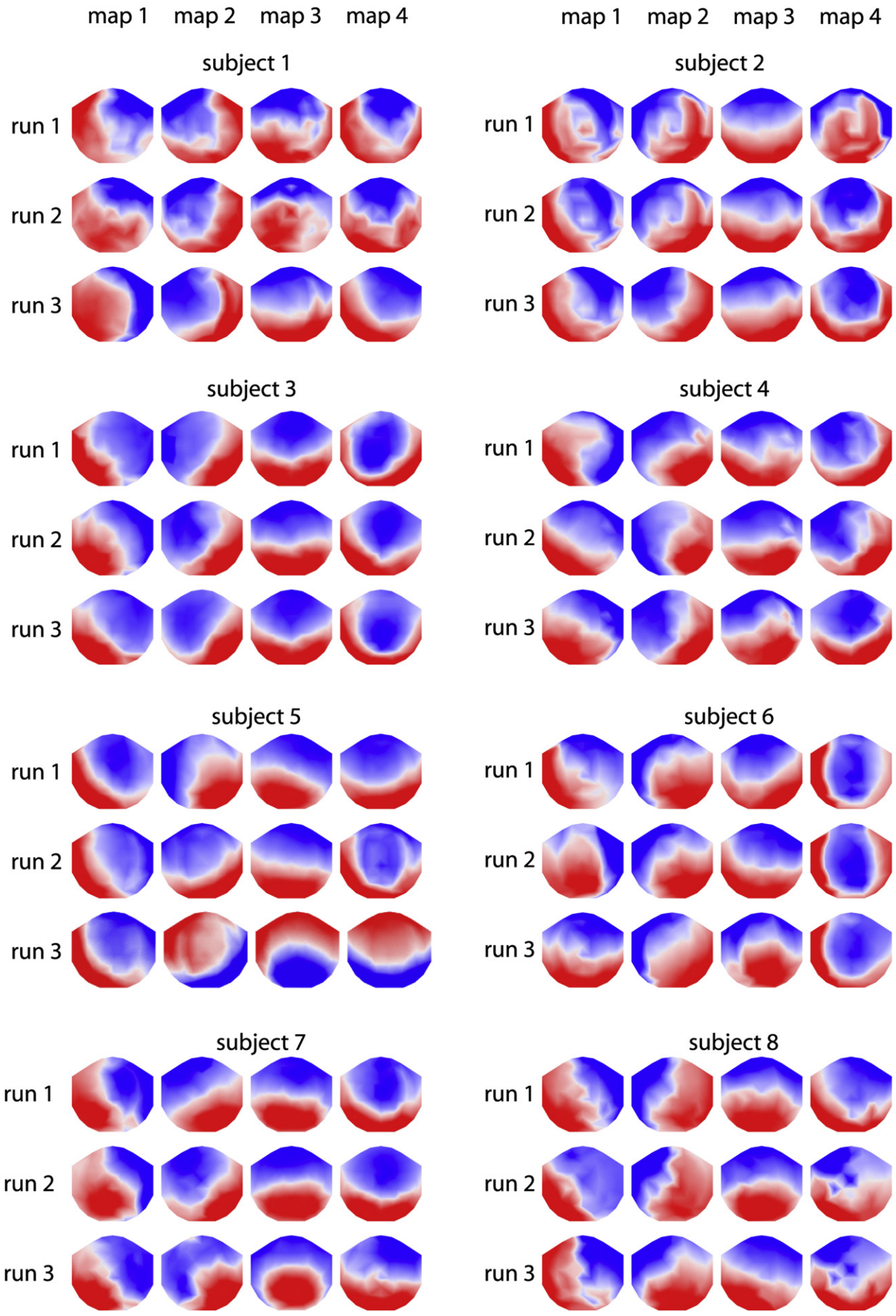
map 1
map 2
map 3
map 4
subject 1
run 1
run 2
run 3
subject 2
subject 3
subject 4
subject 5
subject 6
subject 7
subject 8

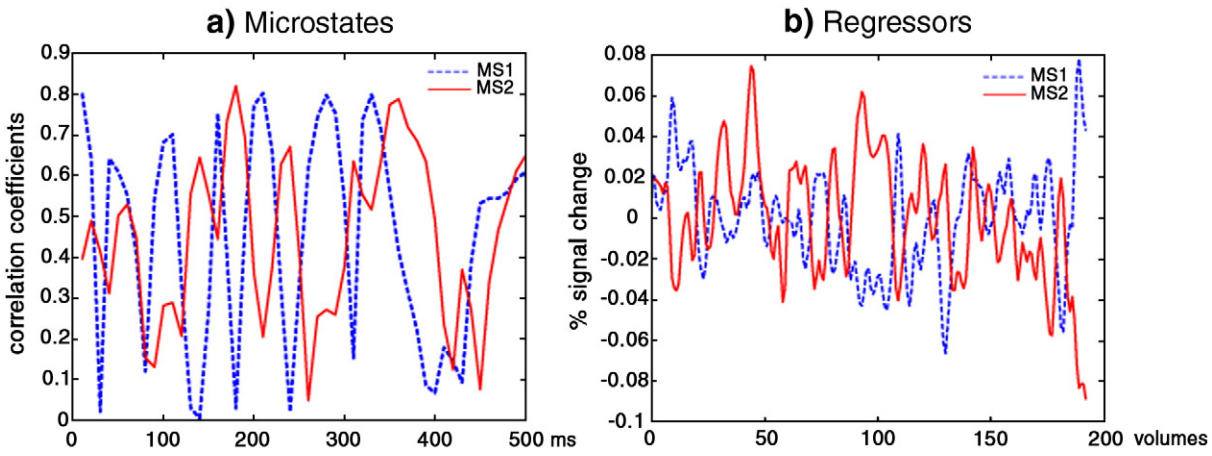

Fig. 2. Scale invariance in the time course of EEG and fMRI signals. a) Time course of the spatial correlation coefficients of MS1 and MS2 in a randomly chosen time interval of 500 ms for one subject; the signals are strongly anti-correlated. b) Time course of the EEG signal after convolution with the HRF for all 200 TRs; the same anti-correlation of time courses is preserved after the convolution, i.e. temporal low-pass filtering.

(Maldjian et al., 2003) as well as the Talairach Demon (Lancaster et al., 2000).

Results

EEG

Identification of the four prototypical EEG microstates

We identified microstates by their map topography. We applied a cluster analysis to the artifact-corrected EEG and used a cross-validation criterion to determine the most dominant topographies. Four template maps yielded the optimal number of clusters in each run for each subject and across all subjects; they explained on average 66.16% (STD = 8.1%, min = 49%, max = 81%) of the overall variance. In the second cluster analysis across all subjects, the cross-validation criterion identified again four templates as the best solution which explained 78% of the variance. Spatial correlation between these templates identified at the group level and those identified at the individual subject level revealed that each template could be identified in each subject in each run. The results of this analysis are displayed in Fig. 1. For further details on their Global Explained Variance and Frequency of Occurrence, see Supplementary Tables 1 and 2. The four microstate maps have strikingly similar topographies across subjects and resemble those described in previous studies (Koenig et al., 2002; Lehmann et al., 2009; Wackermann et al., 1993). Map 1 has a left posterior–right anterior orientation, Map 2 has a right posterior–left anterior orientation, Map 3 has an anterior–posterior orientation and Map 4 has a central maximum. None of the maps were correlated with cardiac activity (see Supplementary Fig. 3).

Fig. 2a shows the time course of the spatial correlations for two microstate maps in one representative subject. The figure confirms the notion of microstates: the time courses are largely anti-correlated, and one map is dominant during a certain time in the sub-second range, interrupted by short transition periods.

Microstates are independent of EEG frequency power

The occurrence of the microstate maps is independent from the power in the five major EEG frequency bands (Fig. 3): we found no correlations between the time courses of the occurrence of map topographies and power in the five EEG frequency bands (mean correlation = 0.021, range −0.006 to 0.112). Moreover, the time courses of map occurrences were also not correlated between each other (mean = 0.094, range −0.357 to 0.375) unlike those of the EEG frequency bands, which showed a positive correlation throughout (mean = 0.448, range 0.314–0.695), this pattern was found in each subject (Supplementary Fig. 2).

fMRI

Results of the GLM analysis

We derived regressors for the BOLD estimation by convolving the time course of the spatial correlation coefficients for each template map with the canonical HRF. Fig. 2b displays the time course of the convolved signal for Microstate Maps 1 and 2 in one subject. It indicates that also at this slower time scale, temporal anti-correlations between the microstate-informed regressors remain.

Fig. 4 displays the fMRI activations along with templates of the microstate maps that were used for their estimation, and foci of activations are summarized in Supplementary Table 3. RSN 1 identified by Map 1 explains a widespread cluster of activations primarily in bilateral superior and middle temporal gyri as well as the left middle frontal gyrus (Fig. 4a). RSN 2 identified by Map 2 explains bilateral activation restricted to bilateral occipital areas in bilateral inferior occipital gyri, bilateral cuneus and the left lingual and middle

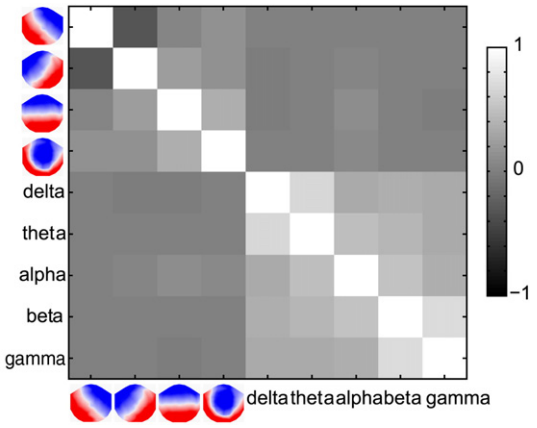

Fig. 3. Correlation matrix of the time courses of the spatial correlation coefficients of the microstate maps and the power in the 5 EEG frequency bands. Power time courses in the EEG frequency bands are positively correlated. Time courses of microstate maps are partly negatively and partly positively correlated. Microstates and frequencies are not correlated.

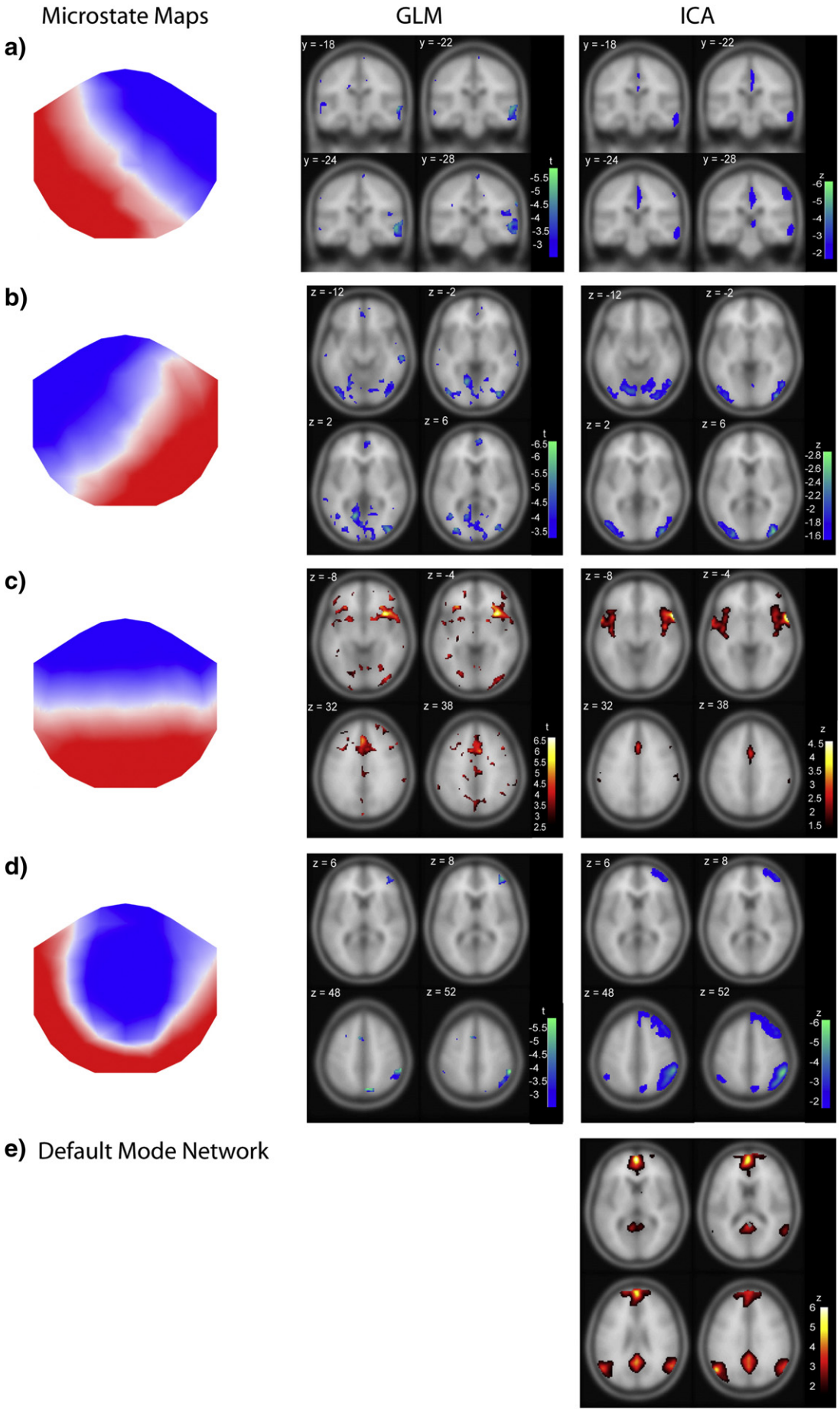
Microstate Maps
GLM
ICA
a)
y = -18
y = -22
y = -24
y = -28
t
-5.5
-5
-4.5
-4
-3.5
-3
z
-6
-5
-4
-3
-2
b)
z = -12
z = -2
z = 2
z = 6
t
-6.5
-6
-5.5
-5
-4.5
-4
-3.5
z
-2.8
-2.6
-2.4
-2.2
-2
-1.8
-1.6
c)
z = -8
z = -4
z = 32
z = 38
t
6.5
6
5.5
5
4.5
4
3.5
3
2.5
z
4.5
4
3.5
3
2.5
2
1.5
d)
z = 6
z = 8
z = 48
z = 52
t
-5.5
-5
-4.5
-4
-3.5
-3
z
-6
-5
-4
-3
-2
e) Default Mode Network
z
6
5
4
3
2

occipital gyrus (Fig. 4b). RSN 3 identified by Map 3 explains bilateral activations in the anterior cingulate cortex and the cingulate gyrus medially and left inferior frontal gyrus and left claustrum as well as the right inferior frontal gyrus and right amygdala (Fig. 4c). RSN 4 identified by Map 4 explains activation in a dorsal network that is primarily right-lateralized and which encompasses the right superior and middle frontal gyrus as well as the right superior and inferior parietal lobules (Fig. 4d). The respective glass brain views are depicted in Supplementary Fig. 4.

These networks were also found by the statistical analysis at the single-subject level, however, not every network was statistically significant in every individual, indicating that the group-level statistics were not driven by a single individual.

Results of the group ICA analysis

Out of the 20 estimated independent components (ICs), five represented noise with activations in the ventricles and at the edges. The remaining 15 ICs corresponded to those previously identified (Beckmann et al., 2005; Calhoun et al., 2008; Damoiseaux et al., 2006; Mantini et al., 2007). Four ICs were found that each correlates significantly with one of the EEG-informed GLM estimations (Fig. 4): one IC encompassing bilateral temporal areas and primary visual areas correlated with the network corresponding to Map 1 ($r=0.38$) (Fig. 4a), one IC encompassing bilateral lateral extrastriate visual areas correlated with the network corresponding to Map 2 ($r=0.58$) (Fig. 4b), one IC encompassing the ACC and bilateral inferior frontal areas correlated with the network corresponding to Map 3 ($r=0.44$) (Fig. 4c), and the IC encompassing right-lateralized frontal and parietal areas correlated with the network corresponding to Map 4 ($r=0.47$) (Fig. 4d). Furthermore, one IC was found to represent the DMN (Fig. 4e). However, no EEG map was correlated with this DMN ICA component.

Discussion

We hypothesized that RSN dynamics are much faster than hemodynamic fluctuations alone suggest and that the EEG microstates are their electrophysiological signature. We used the time course of the EEG microstates indexed by their scalp topography to analyze spontaneous activity in BOLD fMRI. The time course of EEG microstates is of non-hemodynamic origin and a direct measurement of all concurrent synchronized post-synaptic neural activity independent of frequency and is sampled at its original high temporal resolution. The cluster analysis of the EEG topography recorded in the scanner revealed the repeatedly described four dominant map topographies that explained close to 70% of the variance in the data (Koenig et al., 2002; Strik and Lehmann, 1993; Wackermann et al., 1993), the so-called EEG microstates. They were identified as the best solution of the cluster analysis without any a-priori assumptions on the number of clusters or on the minimum of explained variance. The four microstates were de-correlated in time and temporally discontinuous and could be parsed into periods of around 100 ms during which always one of them dominated. These observations are fully in line with the EEG-microstate model (Lehmann et al., 2009), and demonstrate that these microstates can be identified in the EEG recorded in the scanner. The convolution of the time course of each microstate map with the hemodynamic response function revealed highly significant distinct networks of activation. The correlation of these BOLD maps with the networks identified by the independent component analysis of the fMRI revealed one distinct correlating IC map for each microstate-derived BOLD map.

RSN 1 identified by Microstate Map 1 was correlated with negative BOLD activations primarily in bilateral superior and middle temporal gyri, areas that are implicated in phonological processing. It was spatially correlated best with an IC which shows negative BOLD activation in the same temporal areas and additionally in primary visual areas. Very similar networks were identified by means of ICA by Mantini et al. (2007), (RSN 4) and Damoiseaux et al. (2006), (RSN 'G') and were interpreted as reflecting phonological processing. RSN 2 identified by Microstate Map 2 was correlated with negative BOLD in bilateral extrastriate visual areas, BA18 and BA19. It was best correlated with an IC that likewise shows negative BOLD signal in the same extrastriate visual areas. This was previously identified as the visual network RSN 3 in Mantini et al. (2007) and 'E' in Damoiseaux et al. (2006).

RSN 3 identified by Microstate Map 3 was correlated with positive BOLD activations in the posterior part of the anterior cingulate cortex as well as bilateral inferior frontal gyri, the right anterior insula and the left claustrum. It was best correlated with an IC that shows positive BOLD in the ACC and bilateral inferior frontal gyri as well as the insula. It roughly corresponds to RSN 6 in Mantini et al. (2007). The fronto-insular cortex has been found to be part of the saliency-network (Fox et al., 2006; Seeley et al., 2007) and to play a critical role in switching between central-executive function and the default mode (Sridharan et al., 2008). We only find activity in the anterior part of the right insula which has been recently found to be functionally connected to the posterior anterior cingulate cortex and anterior middle cingulate cortex at rest. This connectivity is thought to integrate interoceptive information with emotional salience to form a subjective representation of the own body (Taylor et al., 2009a).

RSN 4 identified by Microstate Map 4 was correlated with negative BOLD signal in right-lateralized dorsal and ventral areas of frontal and parietal cortex. It was correlated with an IC showing negative BOLD in virtually the same frontal and parietal areas. This corresponds to the RSN 2 network in Mantini et al. (2007) and RSN 'C' in Damoiseaux et al. (2006). Ventral fronto-parietal areas subserve reflexive aspects of attention such as detecting behaviorally relevant stimuli while more dorsal areas in fronto-parietal cortex are involved in switching and reorientation of attention (Corbetta and Shulman, 2002).

The neuronal activity reflected by each of these four maps has its idiosyncratic hemodynamic counterpart, i.e. the EEG microstates reflect BOLD signal changes in distinct networks. Previous attempts to relate these networks to activity in the power of discrete EEG frequency bands showed no distinct relation to one single frequency (Mantini et al., 2007). This is confirmed by our comparison of the microstate time course with the time course of the different frequency bands using time-frequency analysis. No correlation was found between the microstates and the different frequency bands, while the different frequency bands correlated among each other. The tight phase-amplitude coupling between the different EEG frequency bands probably underlies these correlations (Schroeder and Lakatos, 2009a,b). These and our results indicate that EEG frequency oscillations are not the electrophysiological signature for the fMRI-defined resting states. The EEG microstates seem to show much more distinct correlations with the fMRI resting states.

Fig. 4. EEG template maps identified at the group level and BOLD activations revealed by GLM and ICA. a) Microstate 1 group-level template map, BOLD activations revealed by GLM regression of its time course and the corresponding correlated IC spatial map were located in bilateral temporal areas. b) Microstate 2 group-level template map, BOLD activations revealed by GLM regression of its time course and correlated IC spatial map were located in bilateral extrastriate visual areas. c) Microstate 3 group-level template map, BOLD activations revealed by GLM regression of its time course and correlated IC spatial map were located in the ACC and bilateral inferior frontal areas. d) Microstate 4 group-level template map, BOLD activations revealed by GLM regression of its time course and correlated IC spatial map were located in right superior and middle frontal gyri as well as the right superior and inferior parietal lobules. e) IC revealed for the DMN.

In is important to note that the sign of the BOLD contrasts revealed by the GLM analysis and in the ICA is always the same: RSNs 1, 2 and 4 show negative BOLD contrasts and RSN 3 shows a positive BOLD contrast. Likewise, the ICs they were best correlated with also showed *z*-scores with the same sign. However, negative BOLD does not necessarily mean de-activation relative to a baseline or decreased neuronal activity which is due to the complex neuron–vascular coupling (Logothetis et al., 2001). Epileptic spikes which unequivocally represent an increase in synchronized neuronal activity can likewise be associated with positive and negative BOLD in the locus of the epileptic focus (Gotman, 2008; Vulliemoz et al., 2009).

The rapid dynamics of the EEG microstates and the fact that their relative temporal correlation is not abolished by the convolution with the HRF indicate that the underlying dynamics of RSNs is much faster than analysis of the fMRI signal alone suggests. Moreover, this measure of momentary overall brain activity varies at a high frequency and is still meaningful after convolution with the HRF. Without the presence of long-range dependencies in the microstate occurrences, convolution with the HRF that acts as a strong temporal smoothing filter would remove any information-carrying signal. The fact that it shows the same relative behavior at time scales that are two orders of magnitude apart is indicative of potentially underlying scale invariance in the time course of microstate presence.

This fast sub-second dynamics of the resting-state networks is intuitively more compatible with the idea of rapidly changing spontaneous cognitive operations. Large-scale networks link groups of neurons in separate cortical areas into functional entities, thereby mediating complex mental activities (Bressler, 1995; Fuster, 2006; Seeley et al., 2009). These large-scale neuronal networks have to grant both stability and plasticity and therefore have to flexibly and rapidly change depending on the momentary cognitive process (Bressler, 1995; Bressler and Tognoli, 2006; Grossberg, 2000). It is therefore required that they reorganize in different spatial patterns of coordination on a sub-second time scale. While this demand is obvious when the brain processes external information, it is reasonable to assume that this fast rearrangement of large-scale neurocognitive networks also takes place during spontaneous mental activity, i.e. during stimulus-independent thoughts.

The large-scale neurocognitive networks might correspond to the proposed “neuronal workspace” that consists of a distributed set of cortical neurons that form a discrete spatiotemporal pattern of activity (Baars, 1997; Dehaene and Naccache, 2001). The neuronal workspace model proposes that episodes of coherent activity last for 100 ms and that are separated by sharp transitions. Only one such workspace representation is active at any given time (Baars, 2002; Dehaene et al., 2003). The segmentation of the EEG into microstates fits this global workspace model. The EEG microstates are a candidate electrophysiological correlate for the process of global integration of local processes at the brain-scale level, which ultimately leads to conscious thought (Changeux and Michel, 2004). It suggests that conscious cognitive processing occurs through a stream of discrete units or epochs rather than as a continuous flow of neuronal activity, i.e. that mental activity evolves through a sequence of quasi-stable coordination states (Fingelkurts and Fingelkurts, 2006; Grossberg, 2000).

The regressors derived from the EEG microstates identified four RSNs that were identified previously, but not the DMN. We identified the DMN by ICA, but we did not identify its neurophysiological signature. Two distinct ideas prevail about the functional significance of intrinsic brain activity (Raichle and Snyder, 2007), i.e. activity at rest in the absence of stimuli and tasks: the notion of stimulus-independent thoughts (Mason et al., 2007) and that of a more fundamental property of intrinsic brain functional organization. Our data suggest that the microstates reflect stimulus-independent thoughts and the default mode a more fundamental property of intrinsic brain organization. The former is supported by the idea that subjects inevitably engage in some kind of unconstrained cognitive activity while being scanned at rest but awake; the kinds of ‘mental operations’ are reflected in the nature of the functional networks identified with the EEG-informed regressors: visual, phonological, introspection and reorienting attention. The latter is supported by the fact that the main nodes of the DMN are already present at birth (Fransson et al., 2007) and that they form the main nodes of the structural core of the cerebral cortex (Hagmann et al., 2008). Moreover, the DMN can also be identified in sleep and coma (Boly et al., 2008) and the anesthetized monkey (Vincent et al., 2007).

Taken together, our results suggest that large-scale networks can be segregated at rest by means of EEG microstates. The time courses of the microstates correlate with BOLD activation in distinct distributed networks. The signal used to construct the regressors for BOLD estimation is of purely neuronal and non-hemodynamic origin. It is sampled at a high temporal resolution and is still meaningful after convolving it with the HRF, which serves as a massive temporal filter. This study is the first that has distinguished four different networks, with a regressor derived from a purely neurophysiological signal sampled with a high temporal resolution. The nature of the regressor suggests that these networks alternate faster than conventional resting-state connectivity analyses alone imply.

Acknowledgments

This work was supported in part by the Swiss National Science Foundation (32003B-118315 and PP00P2-123438, DVDV) and in part by the Center for Biomedical Imaging (CIBM) of the Geneva and Lausanne Universities, EPFL, and the Leenaards and Louis-Jeantet Foundations.

The Cartool software (http://brainmapping.unige.ch/Cartool.htm) has been programmed by Denis Brunet from the Functional Brain Mapping Laboratory, Geneva, Switzerland.

Appendix A. Supplementary data

Supplementary data associated with this article can be found, in the online version, at doi:10.1016/j.neuroimage.2010.02.052.

References

Allen, P.J., Polizzi, G., Krakow, K., Fish, D.R., Lemieux, L., 1998. Identification of EEG events in the MR scanner: the problem of pulse artifact and a method for its subtraction. Neuroimage 8, 229–239.

Allen, P.J., Josephs, O., Turner, R., 2000. A method for removing imaging artifact from continuous EEG recorded during functional MRI. Neuroimage 12, 230–239.

Baars, B., 1997. In the Theater of Consciousness: The Workspace of the Mind. Oxford University Press, New York.

Baars, B.J., 2002. The conscious access hypothesis: origins and recent evidence. Trends Cogn. Sci. 6, 47–52.

Beckmann, C.F., DeLuca, M., Devlin, J.T., Smith, S.M., 2005. Investigations into resting-state connectivity using independent component analysis. Philos. Trans. R. Soc. Lond., Ser. B: Biol. Sci. 360, 1001–1013.

Bell, A.J., Sejnowski, T.J., 1995. An information-maximization approach to blind separation and blind deconvolution. Neural Comput. 7, 1129–1159.

Biswal, B.B., Yetkin, F.Z., Haughton, V.M., Hyde, J.S., 1995. Functional connectivity in the motor cortex of resting human brain using echo-planar MRI. Magn. Reson. Med. 34, 537–541.

Bollimunta, A., Chen, Y., Schroeder, C.E., Ding, M., 2008. Neuronal mechanisms of cortical alpha oscillations in awake-behaving macaques. J. Neurosci. 28, 9976–9988.

Boly, M., Phillips, C., Tshibanda, L., Vanhaudenhuyse, A., Schabus, M., Dang-Vu, T.T., Moonen, G., Hustinx, R., Maquet, P., Laureys, S., 2008. Intrinsic brain activity in altered states of consciousness. Ann. N. Y. Acad. Sci. 1129, 119–129.

Bressler, S.L., 1995. Large-scale cortical networks and cognition. Brain Res. Rev. 20, 288–304.

Bressler, S.L., Tognoli, E., 2006. Operational principles of neurocognitive networks. Int. J. Psychophysiol. 60, 139–148.

Britz, J., Landis, T., Michel, C.M., 2009. Right parietal brain activity precedes perceptual alternation of bistable stimuli. Cereb. Cortex 19, 55–65.

Buzsaki, G., Draguhn, A., 2004. Neuronal oscillations in cortical networks. Science 304, 1926–1929.

Calhoun, V.D., Adali, T., Pearlson, G.D., Pekar, J.J., 2001. A method for making group inferences from functional MRI data using independent component analysis. Hum. Brain Mapp. 14, 140–151.
Calhoun, V.D., Kiehl, K.A., Pearlson, G.D., 2008. Modulation of temporally coherent brain networks estimated using ICA at rest and during cognitive tasks. Hum. Brain Mapp. 29, 828–838.
Canolty, R.T., Edwards, E., Dalal, S.S., Soltani, M., Nagarajan, S.S., Kirsch, H.E., Berger, M.S., Barbaro, N.M., Knight, R.T., 2006. High gamma power is phase-locked to theta oscillations in human neocortex. Science 313, 1626–1628.
Changeux, J.-P., Michel, C.M., 2004. Mechanisms of neural integration at the brain-scale level. The neuronal workspace and microstate models. In: Grillner, S., Graybiel, A.M. (Eds.), Microcircuits: The Interface Between Neurons and Global Brain Function. MIT Press, Cambridge, MA, pp. 347–370.
Corbetta, M., Shulman, G.L., 2002. Control of Goal-directed and Stimulus-driven Attention in the Brain. Nat. Rev. Neurosci. 3, 201–215.
Damoiseaux, J.S., Rombouts, S.A.R.B., Barkhof, F., Scheltens, P., Stam, C.J., Smith, S.M., Beckmann, C.F., 2006. Consistent resting-state networks across healthy subjects. Proc. Natl. Acad. Sci. USA 103, 13848–13853.
D'Argembeau, A., Collette, F., Van der Linden, M., Laureys, S., Del Fiore, G., Degueldre, C., Luxen, A., Salmon, E., 2005. Self-referential reflective activity and its relationship with rest: a PET study. Neuroimage 25, 616–624.
Dehaene, S., Naccache, L., 2001. Towards a cognitive neuroscience of consciousness: basic evidence and a workspace framework. Cognition 79, 1–37.
Dehaene, S., Sergent, C., Changeux, J.-P., 2003. A neuronal network model linking subjective reports and objective physiological data during conscious perception. Proc. Natl. Acad. Sci. U. S. A. 100, 8520–8525.
Fingelkurts, A., Fingelkurts, A., 2006. Timing in cognition and EEG brain dynamics: discreteness versus continuity. Cogn. Process. 7, 135–162.
Fox, M.D., Snyder, A.Z., Vincent, J.L., Corbetta, M., Van Essen, D.C., Raichle, M.E., 2005. The human brain is intrinsically organized into dynamic, anticorrelated functional networks. Proc. Natl. Acad. Sci. USA 102, 9673–9678.
Fox, M.D., Corbetta, M., Snyder, A.Z., Vincent, J.L., Raichle, M.E., 2006. Spontaneous neuronal activity distinguishes human dorsal and ventral attention systems. Proc. Natl. Acad. Sci. USA 103, 10046–10051.
Fransson, P., Skiöld, B., Horsch, S., Nordell, A., Blennow, M., Lagercrantz, H., Aden, U., 2007. Resting-state networks in the infant brain. Proc. Natl. Acad. Sci. 104, 15531–15536.
Fuster, J.M., 2006. The cognit: a network model of cortical representation. Int. J. Psychophysiol. 60, 125–132.
Goldman, R.I., Stern, J.M., Engel Jr., J., Cohen, M.S., 2002. Simultaneous EEG and fMRI of the alpha rhythm. Neuroreport 13, 2487–2492.
Gotman, J., 2008. Epileptic networks studied with EEG–fMRI. Epilepsia 49, 42–51.
Grossberg, S., 2000. The complementary brain: unifying brain dynamics and modularity. Trends Cogn. Sci. 4, 233–246.
Hagmann, P., Cammoun, L., Gigandet, X., Meuli, R., Honey, C.J., Wedeen, V.J., Sporns, O., 2008. Mapping the structural core of human cerebral cortex. PLoS Biol. 6, e159.
Hampson, M., Peterson, B.S., Skudlarski, P., Gatenby, J.C., Gore, J.C., 2002. Detection of functional connectivity using temporal correlations in MR images. Hum. Brain Mapp. 15, 247–262.
Jann, K., Dierks, T., Boesch, C., Kottlow, M., Strik, W., Koenig, T., 2009. BOLD correlates of EEG alpha phase-locking and the fMRI default mode network. Neuroimage 45, 903–916.
Katayama, H., Gianotti, L., Isotani, T., Faber, P., Sasada, K., Kinoshita, T., Lehmann, D., 2007. Classes of multichannel EEG microstates in light and deep hypnotic conditions. Brain Topogr. 20, 7–14.
Koenig, T., Prichep, L., Lehmann, D., Sosa, P.V., Braeker, E., Kleinlogel, H., Isenhart, R., John, E.R., 2002. Millisecond by millisecond, year by year: normative EEG microstates and developmental stages. Neuroimage 16, 41–48.
Koenig, T., Studer, D., Hubl, D., Melie, L., Strik, W.K., 2005. Brain connectivity at different time-scales measured with EEG. Philos. Trans. Biol. Sci. 360, 1015–1023.
Lakatos, P., Shah, A.S., Knuth, K.H., Ulbert, I., Karmos, G., Schroeder, C.E., 2005. An oscillatory hierarchy controlling neuronal excitability and stimulus processing in the auditory cortex. J. Neurophysiol. 94, 1904–1911.
Lancaster, J.L., Woldorff, M.G., Parsons, L.M., Liotti, M., Freitas, C.S., Rainey, L., Kochunov, P.V., Nickerson, D., Mikiten, S.A., Fox, P.T., 2000. Automated Talairach Atlas labels for functional brain mapping. Hum. Brain Mapp. 10, 120–131.
Laufs, H., Krakow, K., Sterzer, P., Eger, E., Beyerle, A., Salek-Haddadi, A., Kleinschmidt, A., 2003. Electroencephalographic signatures of attentional and cognitive default modes in spontaneous brain activity fluctuations at rest. Proc. Natl. Acad. Sci. USA 100, 11053–11058.
Lehmann, D., 1990. Past, present and future of topographic mapping. Brain Topogr. 3, 191–202.
Lehmann, D., Skrandies, W., 1980. Reference-free identification of components of checkerboard-evoked multichannel potential fields. Electroencephalogr. Clin. Neurophysiol. 48, 609–621.
Lehmann, D., Skrandies, W., 1984. Spatial analysis of evoked potentials in man—a review. Prog. Neurobiol. 23, 227–250.
Lehmann, D., Strik, W.K., Henggeler, B., Koenig, T., Koukkou, M., 1998. Brain electric microstates and momentary conscious mind states as building blocks of spontaneous thinking: I. Visual imagery and abstract thoughts. Int. J. Psychophysiol. 29, 1–11.
Lehmann, D., Pascual-Marqui, R.D., Michel, C.M., 2009. EEG microstates. Scholarpedia 4, 7632.
Leopold, D.A., Murayama, Y., Logothetis, N.K., 2003. Very slow activity fluctuations in monkey visual cortex: implications for functional brain imaging. Cereb. Cortex 13, 422–433.
Llinas, R.R., 1988. The intrinsic electrophysiological properties of mammalian neurons: insights into central nervous system function. Science 242, 1654–1664.
Logothetis, N.K., Pauls, J., Augath, M., Trinath, T., Oeltermann, A., 2001. Neurophysiological investigation of the basis of the fMRI signal. Nature 412, 150–157.
Maldjian, J.A., Laurienti, P.J., Kraft, R.A., Burdette, J.H., 2003. An automated method for neuroanatomic and cytoarchitectonic atlas-based interrogation of fMRI data sets. Neuroimage 19, 1233–1239.
Mantini, D., Perrucci, M.G., Del Gratta, C., Romani, G.L., Corbetta, M., 2007. Electrophysiological signatures of resting state networks in the human brain. Proc. Natl. Acad. Sci. 104, 13170–13175.
Mason, M.F., Norton, M.I., Van Horn, J.D., Wegner, D.M., Grafton, S.T., Macrae, C.N., 2007. Wandering minds: the default network and stimulus-independent thought. Science 315, 393–395.
McKeown, M.J., Sejnowski, T.J., 1998. Independent component analysis of fMRI data: examining the assumptions. Hum. Brain Mapp. 6, 368–372.
Mohr, C., Michel, C.M., Lantz, G., Ortigue, S., Viaud-Delmon, I., Landis, T., 2005. Brain state-dependent functional hemispheric specialization in men but not in women. Cereb. Cortex 15, 1451–1458.
Murray, M., Brunet, D., Michel, C., 2008. Topographic ERP analyses: a step-by-step tutorial review. Brain Topogr. 20, 249–264.
Nir, Y., Mukamel, R., Dinstein, I., Privman, E., Harel, M., Fisch, L., Gelbard-Sagiv, H., Kipervasser, S., Andelman, F., Neufeld, M.Y., Kramer, U., Arieli, A., Fried, I., Malach, R., 2008. Interhemispheric correlations of slow spontaneous neuronal fluctuations revealed in human sensory cortex. Nat. Neurosci. 11, 1100–1108.
Pascual-Marqui, R.D., Michel, C.M., Lehmann, D., 1995. Segmentation of brain electrical activity into microstates: model estimation and validation. IEEE Trans. Biomed. Eng. 42, 658–665.
Patel, R.S., Van De Ville, D., DuBois Bowman, F., 2006. Determining significant connectivity by 4D spatiotemporal wavelet packet resampling of functional neuroimaging data. Neuroimage 31, 1142–1155.
Raichle, M.E., Snyder, A.Z., 2007. A default mode of brain function: a brief history of an evolving idea. Neuroimage 37, 1083–1090.
Schroeder, C., Lakatos, P., 2009a. The gamma oscillation: master or slave? Brain Topogr. 22, 24–26.
Schroeder, C.E., Lakatos, P., 2009b. Low-frequency neuronal oscillations as instruments of sensory selection. Trends Neurosci. 32, 9–18.
Seeley, W.W., Menon, V., Schatzberg, A.F., Keller, J., Glover, G.H., Kenna, H., Reiss, A.L., Greicius, M.D., 2007. Dissociable intrinsic connectivity networks for salience processing and executive control. J. Neurosci. 27, 2349–2356.
Seeley, W.W., Crawford, R.K., Zhou, J., Miller, B.L., Greicius, M.D., 2009. Neurodegenerative diseases target large-scale human brain networks. Neuron 62, 42–52.
Sridharan, D., Levitin, D.J., Menon, V., 2008. A critical role for the right fronto-insular cortex in switching between central-executive and default-mode networks. Proc. Natl. Acad. Sci. 105, 12569–12574.
Steriade, M., 2001. Impact of network activities on neuronal properties in corticothalamic systems. J. Neurophysiol. 86, 1–39.
Strik, W., Lehmann, D., 1993. Data-determined window size and space-oriented segmentation of spontaneous EEG map series. Electroencephalogr. Clin. Neurophysiol. 87, 169–174.
Taylor, K.S., Seminowicz, D.A., Davis, K.D., 2009a. Two systems of resting state connectivity between the insula and cingulate cortex. Hum. Brain Mapp. 9999 NA.
Taylor, K.S., Seminowicz, D.A., Davis, K.D., 2009b. Two systems of resting state connectivity between the insula and cingulate cortex. Hum. Brain Mapp. 30, 2731–2745.
Tibshirani, R., Walther, G., 2005. Cluster validation by prediction strength. J. Comput. Graph. Stat. 14, 511–528.
Tyvaert, L., LeVan, P., Grova, C., Dubeau, F., Gotman, J., 2008. Effects of fluctuating physiological rhythms during prolonged EEG–fMRI studies. Clin. Neurophysiol. 119, 2762–2774.
Vincent, J.L., Patel, G.H., Fox, M.D., Snyder, A.Z., Baker, J.T., Van Essen, D.C., Zempel, J.M., Snyder, L.H., Corbetta, M., Raichle, M.E., 2007. Intrinsic functional architecture in the anaesthetized monkey brain. Nature 447, 83–86.
Vulliemoz, S., Thornton, R., Rodionov, R., Carmichael, D.W., Guye, M., Lhatoo, S., McEvoy, A.W., Spinelli, L., Michel, C.M., Duncan, J.S., Lemieux, L., 2009. The spatio-temporal mapping of epileptic networks: combination of EEG–fMRI and EEG source imaging. Neuroimage 46, 834–843.
Wackermann, J., Lehmann, D., Michel, C.M., Strik, W., 1993. Adaptive segmentation of spontaneous EEG map series into spatially defined microstates. Int. J. Psychophysiol. 14, 269–283.
Young, C.K., McNaughton, N., 2009. Coupling of theta oscillations between anterior and posterior midline cortex and with the hippocampus in freely behaving rats. Cereb. Cortex 19, 24–40.